International Journal of Electronics and Communication Engineering.
ISSN 0974-2166 Volume 4, Number 4 (2011), pp. 359-371
© International Research Publication House
http://www.irphouse.com

Theoretical Analysis of Linear Active Circular Antenna Array for Beam Steering

Amar Sharma[1], V.K. Pandey[2] and Binod K. Kanaujia[3]

[1]Department of Electronics and Communication Engg.,
College of Engineering Technology, Moradabad-244103, India
E-mail: sharma.amar@rediffmail.com
[2]Department of Electronics and Communication Engg.,
Noida Institute of Engineering and Technology, Greater Noida (U.P.) India
[3]Ambedkar Institute of Technology, Geeta Colony, New Delhi, India

Abstract

The beam steering characteristics of a 1×4 linear Gunn-integrated active circular antenna array is investigated by varying the bias voltages of the different elements in the array while keeping the side-lobe level 10 dB below the main beam level. By varying the bias voltage of 1st and 4th elements simultaneously, the optimization of beam steering exhibited a beam scanning of 32^0 with 1.912-dB power deviation in main beam.

Introduction

In monolithic implementation of active antennas [1], for every type of component (such as active devices, dc power supply, and control lines), RF distribution network have been integrated at the antenna terminals in order to avoid transition/transmission line losses, which works efficiently as a complete transmitter or receiver in relatively small volume, and exhibit the concept of "distributed oscillator-beam steering" by changing dc bias voltages, that is, without conventional phase shifters [2,3]. Such circuits are very compact, light weight, and very inexpensive; therefore, they are useful in surveillance, security, radar, and communication systems. The elements will be injection locked [4], via mutual coupling. The difference between the self-oscillating frequencies of active antennas can provide a phase shift, which can then be used to electronically scan the beam of the active antenna array.

Until now, the major work reported in this area has been experimental [2,5]. In this work, the author theoretically demonstrated how the bias voltages of 1st and 4th antenna are varied to achieve the maximum beam-steering angle.

Theoretical consideration

Active Gunn-Integrated Circular Patch

The top view of the proposed active Gunn-integrated patch is in figure 1(a). The Gunn diode operates in limited-charge accumulation (LSA) relaxation-oscillator mode [6]. The placement of the Gunn diode [7] is chosen such that the device impedance is matched to the input impedance of the patch. The diode placement location ρ_0 is given by

$$\rho_0 = \frac{F}{\left\{1+\frac{2h}{\pi\varepsilon_r F}\left[ln\left(\frac{\pi F}{2h}\right)+1.7726\right]\right\}^{1/2}}, \quad (1)$$

$$F = \frac{8.791\times10^9}{f_r\sqrt{\varepsilon_r}}$$

where h is the thickness of the substrate, ε_r is the dielectric constant of the substrate, and f_r is the resonant frequency of the antenna at the diode location (equal to the active-device dc resistance).

It is well known that the equivalence circuit of a resonant patch can be represented by a parallel R,L, and C circuits. The values of these parameters are calculated using the cavity model. When the patch is loaded Gunn diode, the equivalent circuit of the Gunn-integrated patch can be given, as shown in figure 1(b)

The effective resonance frequency [7] of the active patch can be obtained as follows:

$$f_r = \frac{1}{\frac{L}{R_0(V/V_T)}+2\pi\sqrt{LC}} \quad (2)$$

where $V$is the dc bias voltage, $V_T$is the threshold voltage, $R_0$is the low-field negative resistance of the device when $V < V_T$,and L is the inductance of the microstrip patch.

The input impedance of Gunn-integrated microstrip patch is obtained according to figure 1(b) as follows:

$$Z_{in} = \frac{\omega_r L^2 R R_d(R_d-R)+j\omega_r L R^2 R_d^2(1-\omega_r^2)}{\left[RR_d(1-\omega_r^2 L(C+C_d)\right]^2+[\omega_r L(R_d-R)]^2} \quad (3)$$

and the reflection coefficient can be given by:

$$\Gamma = (Z_{in} - Z_0)/(Z_{in} + Z_0) \quad (4)$$

where Z_0 = 8Ω (device resistance) the return loss is given by:

$$RL = 20log_{10}|\Gamma| \quad (5)$$

The theoretical radiated E-plane far field of the patch is given by:

$$E_{(\varphi)} = j\frac{k_0 a_e V_0 e^{-jk_0 r}}{2r}[J'_{02}] \quad (6)$$

where

$$J'_{02} = J_0(k_0 a_e sin\varphi) - J_2(k_0 a_e sin\varphi)$$

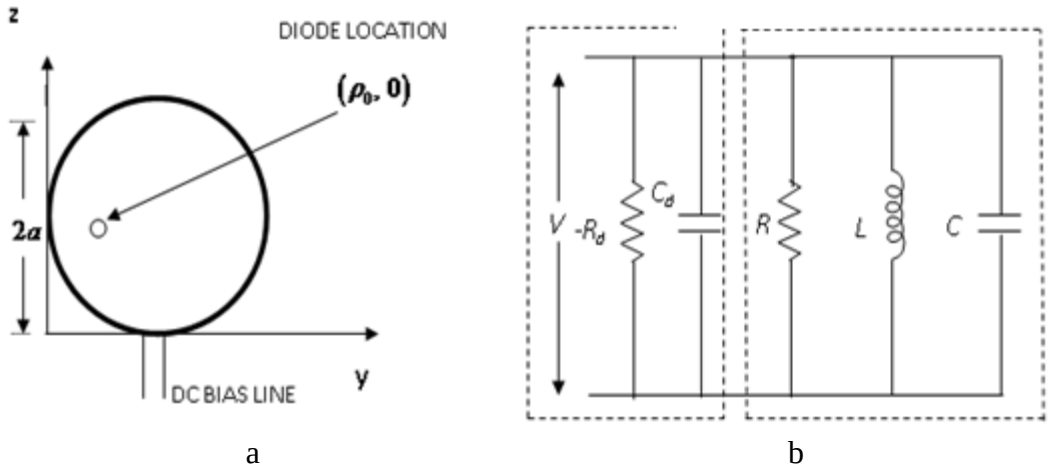

a b

Figure 1: a. Top view of the Gunn integrated microstrip patch with location of diode placement. b. A simplified equivalent circuit of the Gunn-Integrated microstrip patch.

Active Antenna Array

The characteristics of an antenna in the array are different from its characteristics when there is no element in its proximity. These antenna characteristics are called in-place characteristics. Let us consider a microstrip antenna with its input impedance equal to its self impedanceZ_{11}.

If another microstrip antenna is brought in its proximity and its parasitic, then the first element induces current in the second element, and the radiated fields from the second element effect the current distribution in the first element. If the second element is also excited, then the first element will also be affected by direct radiation from the second element. This interchange of energy can be represented by mutual impedance Z_{12} or Z_{21}.For linear and reciprocal elements $Z_{12} = Z_{21}$, they can be calculated as given by[9] . If the element are identical, then $Z_{11} = Z_{22}$.

Table 1: Circular Microstrip Patch.

Substrate Material Used	RT/Duriod 5880
Relative dielectric constant (ε_r)	2.2
Substrate thickness (h)	1.588mm
Center design frequency	10 GHz

Let us consider the 1×4 array shown in Figure 2,in which all elements are placed in the y-z plane, along the y-axis with inter-element spacing of d and angle ϕ measured from x-axis. The in-place radiated far field of antenna 2,3 and 4 work as parasitic elements, is given by:

$$E_{T1} = E_1 \left\{ e^{-jk_1 r} + \frac{Z_{12}}{Z_{22}} e^{-jk_1(r-dsin\varphi)} + \frac{Z_{13}}{Z_{33}} e^{-jk_1(r-2dsin\varphi)} + \frac{Z_{14}}{Z_{44}} e^{-jk_1(r-3dsin\varphi)} \right\} \quad (7)$$

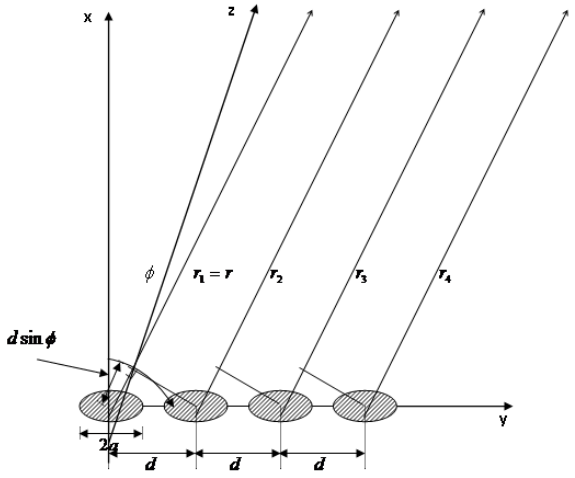

Figure 2: Linear 1x4 active antenna array (y-z plane).

The second, third, and fourth terms in the right-hand side of the above equation represent the field contributed by antennas 2,3 and 4, respectively, due to induced current. When elements 2,3, and 4 are also excited, the resultant field of antenna 1 at far point can be modified as follows:

$$E_{T1} = E_1 \left\{ e^{-jk_1 r} + \frac{Z_{12}}{Z_{22}} e^{-jk_1(r-dsin\varphi)} + \frac{Z_{13}}{Z_{33}} e^{-jk_1(r-2dsin\varphi)} + \frac{Z_{14}}{Z_{44}} e^{-jk_1(r-3dsin\varphi)} \right\} + \frac{Z_{21}}{Z_{11}} E_2 e^{-jk_2 r} + \frac{Z_{31}}{Z_{11}} E_3 e^{-jk_3 r} + \frac{Z_{41}}{Z_{11}} E_4 e^{-jk_4 r}$$

Where E_1, E_2, E_3, E_4 are the radiated far field and k_1, k_2, k_3, k_4 are the wave numbers of antenna 1,2,3 and 4 respectively. The additional terms in the above equation represent the fields contributed by antennas 2,3 and 4 due to their excitations.

Similarly, for other antennas, the radiated far fields can be written as:

$$E_{T2} = E_2 \left\{ e^{-jk_2(r-dsin\varphi)} + \frac{Z_{21}}{Z_{11}} e^{-jk_2 r} + \frac{Z_{23}}{Z_{33}} e^{-jk_2(r-2dsin\varphi)} + \frac{Z_{24}}{Z_{44}} e^{-jk_2(r-3dsin\varphi)} \right\} + \frac{Z_{12}}{Z_{22}} E_2 e^{-jk_1(r-dsin\varphi)} + \frac{Z_{32}}{Z_{22}} E_3 e^{-jk_3(r-dsin\varphi)} + \frac{Z_{42}}{Z_{22}} E_4 e^{-jk_4(r-dsin\varphi)}$$

$$E_{T3} = E_3\left\{e^{-jk_3(r-2dsin\varphi)} + \frac{Z_{31}}{Z_{11}}e^{-jk_3r} + \frac{Z_{32}}{Z_{22}}e^{-jk_3(r-dsin\varphi)} + \frac{Z_{34}}{Z_{44}}e^{-jk_3(r-3dsin\varphi)}\right\} + \frac{Z_{13}}{Z_{33}}E_1e^{-jk_1(r-2dsin\varphi)} + \frac{Z_{23}}{Z_{33}}E_2e^{-jk_2(r-2dsin\varphi)} + \frac{Z_{43}}{Z_{33}}E_4e^{-jk_4(r-2dsin\varphi)}$$

$$E_{T3} = E_3\left\{e^{-jk_3(r-2dsin\varphi)} + \frac{Z_{31}}{Z_{11}}e^{-jk_3r} + \frac{Z_{32}}{Z_{22}}e^{-jk_3(r-dsin\varphi)} + \frac{Z_{34}}{Z_{44}}e^{-jk_3(r-3dsin\varphi)}\right\} + \frac{Z_{13}}{Z_{33}}E_1e^{-jk_1(r-2dsin\varphi)} + \frac{Z_{23}}{Z_{33}}E_2e^{-jk_2(r-2dsin\varphi)} + \frac{Z_{43}}{Z_{33}}E_4e^{-jk_4(r-2dsin\varphi)}$$

$$E_{T4} = E_4\left\{e^{-jk_4(r-3dsin\varphi)} + \frac{Z_{41}}{Z_{11}}e^{-jk_4r} + \frac{Z_{42}}{Z_{22}}e^{-jk_4(r-dsin\varphi)} + \frac{Z_{42}}{Z_{33}}e^{-jk_4(r-2dsin\varphi)}\right\} + \frac{Z_{14}}{Z_{44}}E_1e^{-jk_1(r-3dsin\varphi)} + \frac{Z_{24}}{Z_{44}}E_2e^{-jk_2(r-3dsin\varphi)} + \frac{Z_{34}}{Z_{44}}E_3e^{-jk_3(r-3dsin\varphi)}$$

For linear, reciprocal, and identical elements, $Z_{12} = Z_{21} = Z_{23} = Z_{32} = Z_{34} = Z_{43} = Z_1, Z_{13} = Z_{31} = Z_{24} = Z_{42} = Z_2$ and $Z_{11} = Z_{22} = Z_{33} = Z_{44} = Z$ (Self-impedance of the antenna Z'_{in}). Then the total radiated far field of array is the vector sum of the above fields, given by:

$$E_{(\varphi)} = E_1e^{-jk_1r}\left\{1 + \frac{2}{Z}\left(Z_1e^{jk_1dsin\varphi} + Z_2e^{jk_12dsin\varphi}\right) + Z_1e^{jk_13dsin\varphi}\right\} + E_2e^{-jk_2r}\left\{e^{jk_2dsin\varphi} + \frac{2}{Z}\left(Z_1 + Z_1e^{jk_22dsin\varphi} + Z_2e^{jk_23dsin\varphi}\right)\right\} + E_3e^{-jk_3r}\left\{e^{jk_32dsin\varphi} + \frac{2}{Z}\left(Z_2 + Z_1e^{jk_3dsin\varphi} + Z_2e^{jk_33dsin\varphi}\right)\right\} + E_4e^{-jk_4r}\left\{e^{jk_43dsin\varphi} + \frac{2}{Z}\left(Z_3 + Z_2e^{jk_4dsin\varphi} + Z_1e^{jk_32dsin\varphi}\right)\right\} \quad (10)$$

where

$$k_n = \frac{2\pi}{c}\left(\frac{1}{\frac{L}{\left(R_0(V_n/V_T)\right)}} + 2\pi\sqrt{LC}\right)$$ for n=1,2,3,4.

Here, V_1, V_2, V_3 and V_4 are the dc bias voltages of the diodes in antennas 1,2,3 and 4 respectively.

In the design of the array antenna, the spacing between the elements is a prime factor, which is chosen based upon the coupling requirements for injection locking.

Table 2: Gunn Diode(M/A Comm 49104, GaAs, n).

Diode Resistance	8Ω
Threshold voltage	(2.9 – 4.4)V
Operating point I_0at V_b mA/V	200 at 9.0 V
Oscillating frequency(X-band)	(8.0-12.4)GHz
Operating mode	LSA relaxation mode
Output power mW(>25cw) 10-25mW at	10GHz
Conversion efficiency	(2-5)%
Device capacitance (Cd)	0.1 pF
Typical value of Low-field Resistance (-R_0)	-13.97Ω
Typical value of device negative Resistance	-200Ω
dc bias voltage	(8.0-15.0)V

The typical experimental data given by Kai Chang, K.A. Hummer, and J.A. Klein[4] shows that for 27.9 MHz tuning, BW gain of 25dB is required and bandwidth of this order of gain, which is obtainable via mutual coupling, an edge separation between the element of the order of 0.35λ will be required [10]. This makes the element spacing d (center to center) equal to λ.

Design Specification and Calculations

The design specifications of the circular microstrip patch and the Gunn diode are given in Tables 1 and 2 respectively. The designed parameters of the active patch and the array are shown in Table 3.

Table 3: Designed Parameters of the Active Patch and the Array.

ρ_0 =0.042mm	L=1.1766pH
a=5.25mm	R=8.364Ω
C=2.1629pF	

Discussion of Results

Variation of the resonance frequency with bias voltage for threshold voltages 2.9 V and 4.4 V is shown in Figure 3. It is observed that the resonance frequency decreases with bias voltage, and the tuning bandwidth for the lower threshold voltage (V_T= 2.9 V) is considerably low (14.2 MHz), as compared to the tuning bandwidth (21.7 MHz) at higher threshold voltage (V_T= 4.4 V). The variation of return loss with bias voltage is shown in Figure 4. It can be observed, that there is no significant variation in the return loss, indicating almost matched condition for the entire range of the bias voltage.

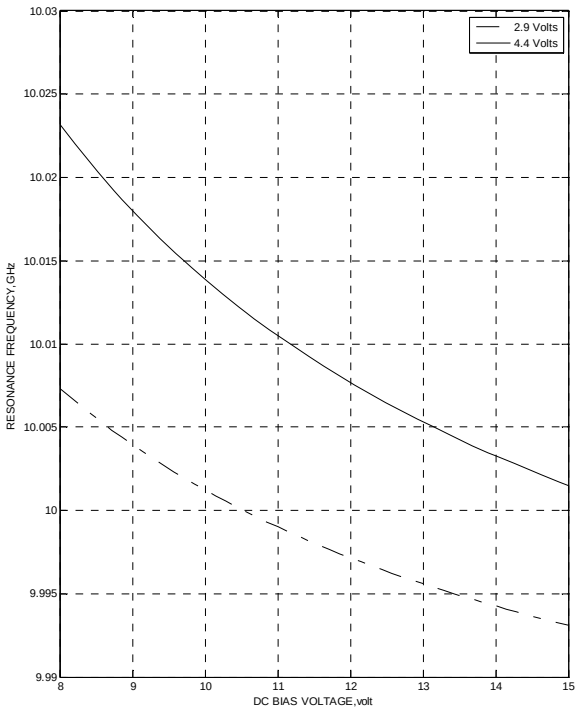

Figure 3: Variation of resonance frequency with dc bias voltage.

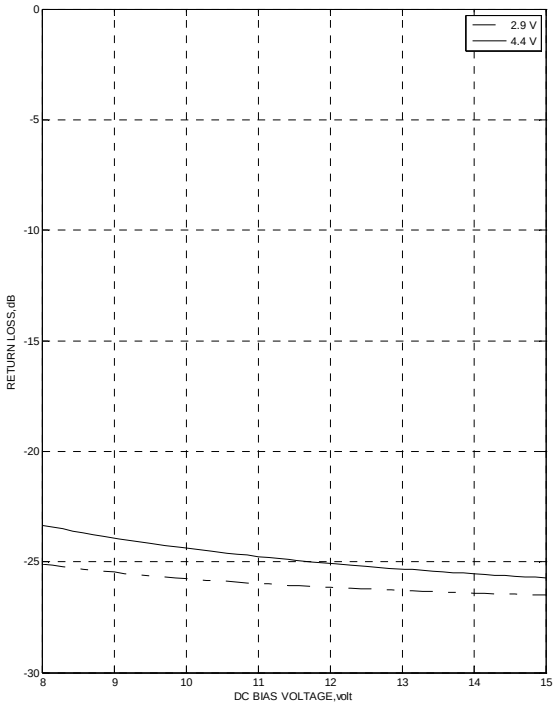

Figure 4: Variation of return loss with bias voltage.

Beam Steering

Case 1: The radiation pattern of the array, as shown in Figure 5 and Figure 6 corresponds to the condition in which the bias voltage $V_1$of the antenna 1 is variable, while the other three elements are kept constant at 10.5326 V. This means that the frequency of the element 1 is variable with bias voltage V_1 ,while the frequency of antenna 2, 3, and 4 are constant at 10.012 GHz. From Figure 5, it shows the decrease in the bias voltage of antenna 1 from 10.5326 V to 10.5298 V gives rise to frequency variation from 10.0120 GHz to 10.0120091 GHz. In this case, in order to achieve the scanning, when bias voltage is lowered from 10.5326 V to 10.5298 V the frequency deviation of 9.1 kHz takes place, and the beam shifts to the left side, that is, the extreme left (-8^0) at 10.0120091 GHz corresponding to bias voltage 10.5298 V.

The further decrease in the bias voltage to 10.5294 V gives rise to the frequency variation to 10.012104 GHz results in increase of side lobe above 10 dB. From Figure 6, it shows the increase in the bias voltage of antenna 1 from 10.5326 V to 10.5354 V gives fall of frequency variation from 10.0120 GHz to 10.0119909 GHz. In this case, in order to achieve the scanning, when bias voltage is increased from 10.5326 V to 10.5354 V the frequency deviation of 9.1 kHz takes place, and the beam shifts to the right side, that is, the extreme right ($+8^0$) at 10.0119909 GHz corresponding to bias voltage 10.5354 V. The further increase in the bias voltage to 10.5358 V gives fall of frequency to 10.0119896 GHz results in increase of side lobe above 10 dB. Hence, the total scan angle achievable in this case is only $16^0(\pm 8^0)$ with relative power loss of 1.712 dB in the main beam

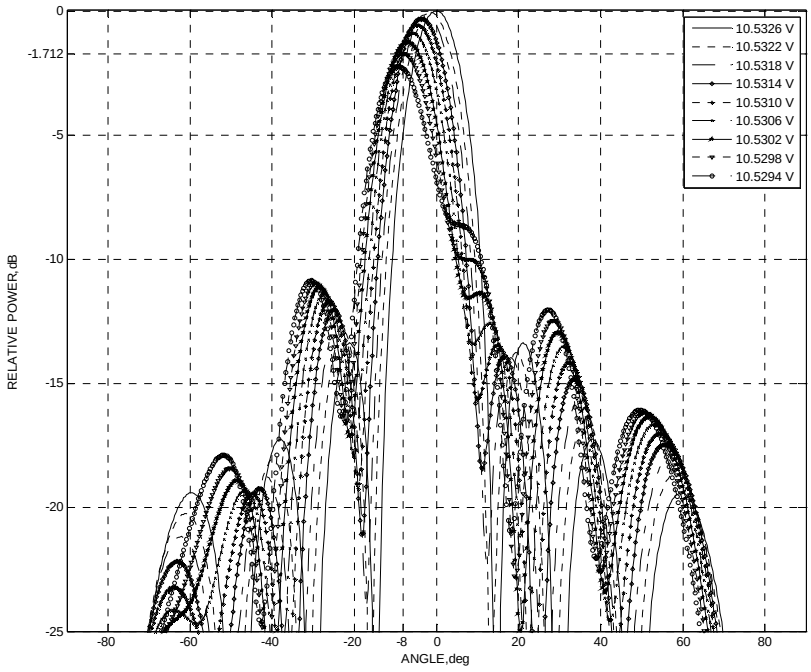

Figure 5: Radiation pattern of active microstrip antenna by decreasing V_1 only [V_2 = V_3 = V_4 = 10.5326 V (10.012 GHz)].

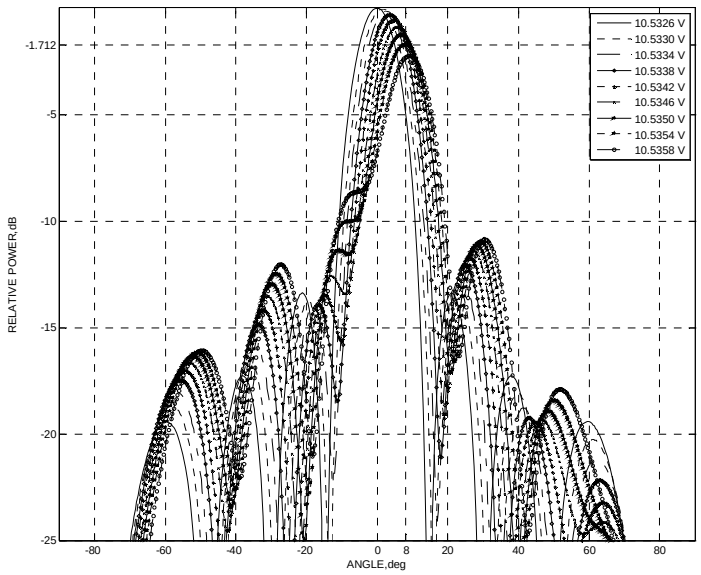

Figure 6: Radiation pattern of active microstrip antenna by increasing V_1 only [$V_2 = V_3 = V_4 = 10.5326\ V$ (10.012 GHz)]

Case 2: The radiation pattern of the array, as shown in Figure 7 and Figure 8 corresponds to the condition in which the bias voltage V_4 of the antenna 4 is variable, while the other three elements are kept constant at 10.5326 V. This means that the frequency of the element 4 is variable with bias voltage V_4, while the frequency of antenna 1, 2 and 3 are constant at 10.012 GHz. From Figure 7, shows the increase in the bias voltage of antenna 4 from 10.5326 V to 10.5354 V gives decrease in frequency variation from 10.0120 GHz to 10.0119909 GHz. In this case, in order to achieve the scanning, when bias voltage is rise from 10.5326 V to 10.5354 V the frequency deviation of 9.1 kHz takes place, and the beam shifts to the left side, that is, the extreme left (-8^0) at 10.0119909 GHz corresponding to bias voltage 10.5354 V. The further increase in the bias voltage to 10.5258 V gives fall in frequency to 10.0119896 GHz results in increase of side lobe above 10 dB. From Figure 8, shows the decrease in the bias voltage of antenna 4 from 10.5326 V to 10.5298 V gives rise to frequency variation from 10.0120 GHz to 10.0120091 GHz. In this case, in order to achieve the scanning, when bias voltage is decreased from 10.5326 V to 10.5298 V the frequency deviation of 9.1 kHz takes place, and the beam shifts to the right side, that is, the extreme right ($+8^0$) at 10.0120091 GHz corresponding to bias voltage 10.5298 V. The further decrease in the bias voltage to 10.5294 V gives rise of frequency to 10.0120104 GHz results in increase of side lobe above 10 dB. Hence, the total scan angle achievable in this case is only $16^0(\pm 8^0)$ with relative power loss of 1.712 dB in the main beam.

After observing the radiation pattern in above two cases, it was thought useful to optimize the scanning characteristic of the array antenna. The bias voltages of 1 and 4 antenna were varied in such a fashion as to obtain the maximum scan angle. The

resulting radiation patterns with values of bias voltages of each antenna are shown in Fig. 3.10. To achieve the left-hand-side scanning, the frequency of antenna 1 is increased while the frequency of antenna 4 is decreased with respect to centre frequency (10.012 GHz). Similarly, for right-hand-side scanning, the frequency of antenna 1 is decreased while the frequency of antenna 4 is increased with respect to centre frequency (10.012 GHz).

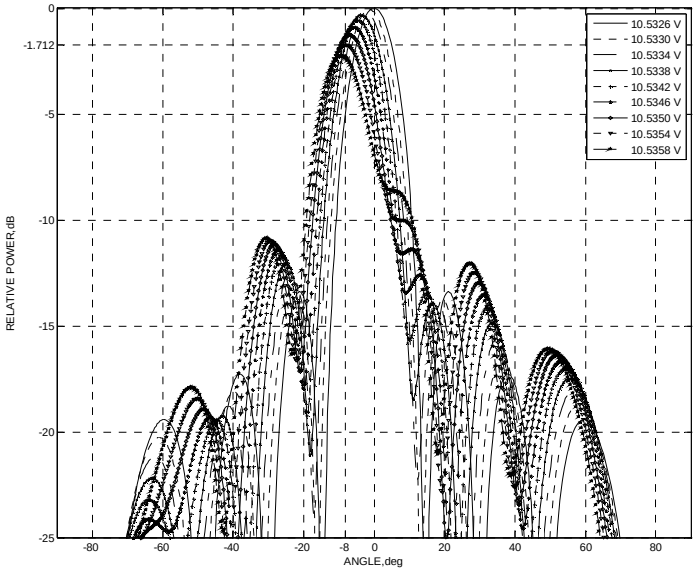

Figure 7: Radiation pattern of active microstrip antenna by increasing V_4 only [V_1 = V_2 = V_3 = 10.5326 *V* (10.012 GHz)]

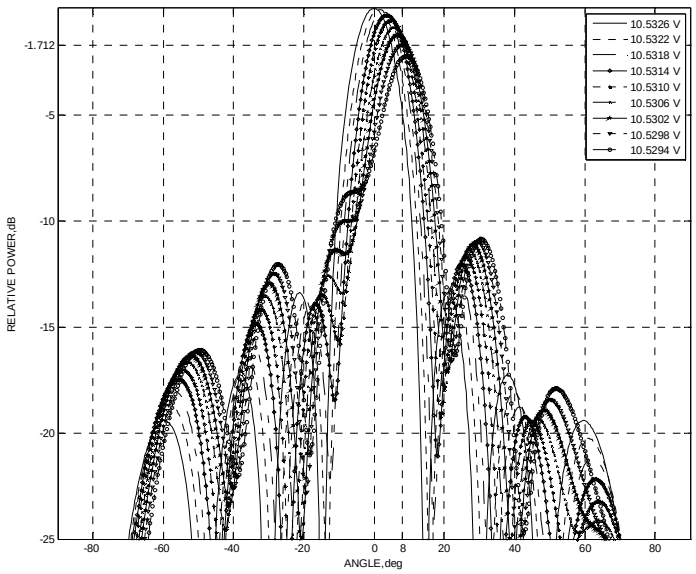

Figure 8: Radiation pattern of active microstrip antenna by decreasing V_4 only [V_1 = V_2 = V_3 = 10.5326 *V* (10.012 GHz)]

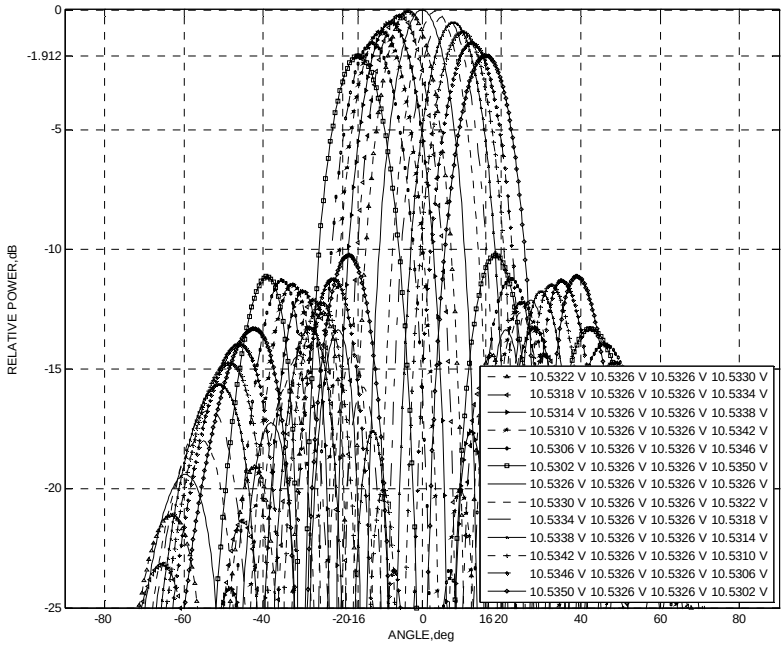

Figure 9: Radiation pattern of active microstrip antenna by changing V_1 and V_4 only [$V_2 = V_3 = 10.5326\ V$ [(10.012 GHz)]

The total frequency deviation of antenna 1 and 4 was ± 7.8 kHz, while the frequency of antenna 2 and 3 was kept constant 10.012 GHz, respectively. The corresponding frequency deviation of the antennas, scan angle, and change in the main-beam relative-power level are given in TABLE 4.

Table 4: Linear 1×4 array frequency distribution for beam scanning.

Antenna 1 f_1 (GHz)	Antenna 2 f_2 (GHz)	Antenna 3 f_3 (GHz)	Antenna 4 f_4 (GHz)	Scan angle (deg)	Change in main beam power level (dB)
10.0120078	10.0120000	10.0120000	10.0119922	-16	1.91200
10.0120065	10.0120000	10.0120000	10.0119935	-13.30	1.37800
10.0120052	10.0120000	10.0120000	10.0119948	-10.64	0.91050
10.0120039	10.0120000	10.0120000	10.0119961	-7.98	0.53050
10.0120026	10.0120000	10.0120000	10.0119974	-5.32	0.24240
10.0120013	10.0120000	10.0120000	10.0119987	-2.66	0.06514
10.0120000	10.0120000	10.0120000	10.0120000	0	0.00
10.0119987	10.0120000	10.0120000	10.0120013	+2.66	0.06514
10.0119974	10.0120000	10.0120000	10.0120026	+5.32	0.24240
10.0119961	10.0120000	10.0120000	10.0120039	+7.98	0.53050
10.0119948	10.0120000	10.0120000	10.0120052	+10.64	0.91050
10.0119935	10.0120000	10.0120000	10.0120065	+13.30	1.37800
10.0119922	10.0120000	10.0120000	10.0120078	+16	1.91200

The approximate expression for the bias voltage of each antenna for a given scan angle can be derived as follows.

From Table 4, it is observed that the scan angle is proportional to the change in the operating frequency of the antennas. It is important to note that the maximum scan angle is achieved when the frequency change of 7.8 kHz is effected in the antenna pair I (antennas 1 & 4), while it is constant for antenna pair II (antenna 2 and 3). The corresponding variation of the bias voltage needs to be from 10.5302 V to 10.5350 V in order to achieve a beam scan angle of 32^0. For this range of bias-voltage, the resonance frequency (Figure 3) depends on the bias voltage which is approximately linear in nature. This indicates that a similar relation will exist between the bias voltages and scan angle. If V is the bias voltage at which the elements are resonant at the centre frequency (10.012 GHz), then the values of the various bias voltages at scan angle θ_{scan} (in degrees) in Equation 10 are given by

$$V_1 = V + \frac{\Delta V_{max}}{\theta_{max}}\theta_{scan}\,, V_2 = 10.5326\,V,$$

$$V_4 = V - \frac{\Delta V_{max}}{\theta_{max}}\theta_{scan}\,, V_3 = 10.5326\,V$$

$$\text{for } -16^0 \le \theta_{scan} \le 16^0 \qquad (11)$$

where∇V_{max} is the maximum change in bias voltage for the maximum scan rangeθ_{max}. The scan angle θ_{scan} is measured from the broad side direction and is taken as negative and positive for the left and right sides in the broadside direction, respectively. The resultant radiation patterns are shown in Figure 9. It is interesting to note that a total beam scanning of $32^0(\pm 16^0)$ is achieved in this case. Similar experimental results were also reported by Navarro and Chang [5], where they used Gunn-integrated inverted strip line circular patches and obtained a beam scanning of 36^0. It is further noted that the maximum change in main beam level during the course of scanning is found to be 1.912 dB while the side lobe level is 10 dB below the main beam.

Conclusion

It may be concluded that the resonance frequency of active antenna decreases with bias voltage, and shows higher tuning bandwidth at higher threshold voltage. Further, it is observed that for maximum scan angle, the bias voltages of antenna pair I (antennas 1 & 4) in 1×4 array should be varied simultaneously

References

[1] J. A. Navarro, K. A. Hummer, and K. Chang, “Active integrated antenna elements,” *Microwave Journal*, pp. 115-127, Jan. 1991.

[2] J. A. Navarro and K. Chang, "Beam steering of active antenna array," *Electron. Lett.*, vol. 29, no. 3, pp. 302-304, Feb. 1993.
[3] W. E. Forsyth and W. A. Shiroma, "A retrodirective antenna array using a spatially fed local oscillator," *IEEE Trans. Antennas Propagat.*, vol. 50, no. 5, pp. 638-640, May 2002.
[4] K. Chang, K. A. Hummer, and J. L. Klein, "Experiments on injection locking of active antenna elements for active phased array and spatial power combiners," *IEEE Trans. Microwave Theory and Tech.*, vol. 37, no. 7, pp. 1078-1084, Jul. 1989.
[5] K. F. Lee and W. Chen, *Advances in microstrip and printed antennas*, John Wiley & Sons, Inc., 1997, pp. 221-222.
[6] S. K. Sharma and Babau R. Vishvakarma, "Gunn integrated microstrip active antenna," *Indian J of Radio & Space Phys*, vol. 26, pp. 40-44, Feb. 1997.
[7] H. J. Thomas, D. L. Fudge, and G. Morris, "Gunn source integrated with microstrip patch," *Microwave and RF*, pp. 87-91, Feb. 1985.
[8] K. R. Carver and J. W. Mink, "Microstrip antenna technology," *IEEE Trans. Antennas Propagat.*, vol. AP-29, no. 1, pp. 2-24, Jan. 1981.
[9] D. R. Jackson, W. F. Richards, and A. Ali-Khan, "Series expansions for the mutual coupling in microstrip patch arrays," *IEEE Trans. Antennas Propagat.*, vol. 37, no. 3, pp. 269-274, Mar. 1989.
[10] D. M. Pozar, "Input impedance and mutual coupling of rectangular microstrip antennas," *IEEE Trans. Antennas Propagat.*, vol. AP-30, no. 6, pp.1191-1195, Nov. 1982.